Title
SCATTERING AND BOUND STATE POTENTIALS IN DWBA CALCULATIONS

Authors
Duhm, K.H.
Hendrie, D.L.
Harvey, B.G.

Publication Date
1967-10-01

UCRL-17883

ey. 2

University of California

Ernest O. Lawrence Radiation Laboratory

SCATTERING AND BOUND STATE POTENTIALS IN DWBA CALCULATIONS

H. H. Duhm, D. L. Hendrie, and B. G. Harvey

October 1967

DISCLAIMER

Submitted to Physics Letters

UCRL-17883
Preprint

UNIVERSITY OF CALIFORNIA

Lawrence Radiation Laboratory
Berkeley, California

AEC Contract No. W-7405-eng-48

SCATTERING AND BOUND STATE POTENTIALS IN DWBA CALCULATIONS

H. H. Duhm, D. L. Hendrie, and B. G. Harvey

October 1967

SCATTERING AND BOUND STATE POTENTIALS IN DWBA CALCULATIONS*

H. H. Duhm,† D. L. Hendrie, and B. G. Harvey

Lawrence Radiation Laboratory
University of California
Berkeley, California

October 1967

ABSTRACT

Optical model potentials appropriate for the description of scattering and reactions in the ^{24}Mg region were investigated.

---

*This work was performed under the auspices of the U. S. Atomic Energy Commission.

†Permanent address: Max Planck Institut für Kernphysik, Heidelberg.

UCRL-17883

Scattering and Bound State Potentials in DWBA Calculations

H. H. Duhm, D. L. Hendrie, and B. G. Harvey
Lawrence Radiation Laboratory, Berkeley, California

Optical model potentials appropriate for the description of scattering and reactions in the ^{24}Mg region were investigated. The scattering potentials were obtained for p, d, ^{3}He and α particles elastically scattered by ^{24}Mg. (E=30.5 MeV, E_p=40 MeV, $E_{^3He}$=35 and 47.5 MeV, E_α=50.1, 65.7, 81 and 119.7 MeV). The resulting parameter families were found to be closely related to the Wood-Saxon bound state potential well depths for the corresponding cluster wave functions of the (^{24}Mg + particle)-system with a proper number of nodes within the nuclear interior. For pickup reactions like ^{24}Mg(d, ^{3}He)^{23}Na and ^{26}Mg(p,t)^{24}Mg the choice of fitting potentials seems to be largely influenced by the sum rule criterion for the real potential, namely $V_{^3He} = V_d^{scatt.} + V_p^{bound}$ and $V_t = V_{2n}^{bound} + V_p^{scatt.}$ (at equal radii). Using V_t according to this sum rule (constructed potential), the ratios of intensities for the ℓ=0 ^{26}Mg(p,t)^{24}Mg transitions to the 14.53 MeV, T=2 state and to the ground state in ^{24}Mg is close to the value expected from pure $(d_{5/2})^n$ configurations.

The proton (neutron) scattering potential is known to be closely connected to the bound state potential. For composite particles the scattering potentials should similarly be chosen in a way that is consistent with a shell model decription of the bound state. In the simplest approach, neglecting interactions between the constituents of the cluster as well as the effect of the cluster on the core, the bound state potential of the composite particle is just the sum of potentials for its nucleons. This sum rule of potentials $V = \langle \sum V_{nucleon} \rangle$ [1] is, of course, in the spirit of zero range approximations used in the distorted wave analysis of elastic scattering [2].

Fig. 1 shows the elastic angular distributions used in our analysis. The 30.5 MeV proton data were taken by Cole et al [3]. The d, ^{3}He and α distributions were obtained at the Berkeley 88-inch cyclotron [4], the α data being measured by Reed [5]. The solid lines are optical model fits using not best fit but 'systematic' parameters of Table 1 (r_o=1.2 F fixed for p, d, ^{3}He and

V=100 MeV fixed for α scattering). In particular, the ^{3}He fits can be improved by using a smaller value of r_o (see Fig. 2). The search code Mercy [6], was used with the usual X^2-criterion. (The errors on the data points were assumed to be either 5% or the statistical errors where they exceeded 5%). Spin orbit potentials were neglected and a volume imaginary potential was used although surface imaginary potentials gave equally good fits for p, d and ^{3}He.

For protons only one V(r,a) family could be found. The next higher family (V≈200, $r_o \simeq 1.0$) does not fit the backward angle cross sections. There is not much change between the proton parameters for 30.5 [3] and 50 [7] MeV bombarding energy. The deuteron angular distribution could be fitted by two parameter families because of the restricted range of measured angles. Other data, e.g. the 52 MeV Karlsruhe data [8], however, exclude the higher 4S deuteron family - again by the backward angle behavior. In the case of ^{3}He the present data can be fitted by different sets of parameters equally well. No significant energy dependence of potentials could be observed. The α potential, however, studied for a larger range of bombarding energies, varied appreciably. At lower bombarding energies the well known ambiguities appear as in the case of ^{3}He. They arise from the surface localization of the interaction, allowing the elastic wave function to have a different number of nodes in the interior of the nucleus [9]. Since the reflection from the real potential significantly contributes to the surface localization at medium bombarding energies one might hope that elastic scattering at higher bombarding energies would become more sensitive to the nuclear interior and the potential ambiguities would be removed. This is in fact what we have observed for the 119.7 MeV scattering data. This potential depth seems to be consistent with the 'right' 5S bound state potential (Table 1, Fig. 2). Tracing back this parameter family to lower bombarding energies, the diffuseness and the value of the product $r_o \cdot a$ decrease, whereas the radius increases (the potential depth does not vary much). If, however, the radius is kept to a fixed value the potential becomes deeper with decreasing bombarding energy. (Our analysis of 42 MeV and 28 MeV α data from Ref. 18 and 19 seems to indicate that the 5S α potential depth may reach a maximum value at a bombarding energy of about 50 MeV).

Fig. 2 shows a map of X^2 valleys in the (V,r_o) plane. All other parameters were left open to adjustment. Mostly 6 parameter potentials were used, where the coupling

between the real and the imaginary part is less strong than for 4 parameter fits. For α scattering 4 parameter best fit regions are also indicated, the numbers giving the value of X^2. Within the best fit valleys lgV is almost proportional to r_o. The real diffuseness "a" is strongly correlated with r_o the value of the product $r_o \cdot a$ being almost constant within one family at a given bombarding energy. This is demonstrated by the comparison of $X^2(r_o)$ for best fit parameters with $X^2(r_o \cdot a = \text{const.})$ for p, d and α potentials. The solid lines are the results of bound state well depth calculations for a different number of nodes using the binding energies E_b of Table 2 and the r_o, a values of the scattering potentials. Only the calculated curve for protons is obtained in a different way. Here we used $V_{cluster}(E_b^{free})$. Dividing $V(E_b^{free})$ by the number of nucleons of the composite particle one obtains a unique curve which compares well with the proton scattering potentials.

The bound state potentials $V_b(E_b)$ of the cluster wave functions are in fair agreement with the scattering potentials $V_{scatt.}$. By varying the number of nodes the different potential families are reproduced. The ^{3}He potentials come closer to the calculated curves at radii smaller than 1 Fermi. This may explain the small best fit radii for the real part of the ^{3}He potential.

Our calculations of bound state potentials (code Julie)[10] are based on the assumption that cluster wave functions with a proper number of nodes within the nuclear interior yield reasonable well depths for the corresponding (target nucleus + particle)-system. Expanding an n-particle shell model configuration in terms of a center of mass and a relative motion, the cluster term, where all nucleons are in a relative ls state is, of course, usually far less than 50% of the total wave function (see Moshinsky brackets for a two particle system within a harmonic oscillator potential)[11]. In an unperturbed many particle system, however, all these components are degenerate yielding the same energy in terms of oscillator quanta.

According to the cluster model the center of mass motions for the $(2s,1d)^n$ configurations of the (^{24}Mg + particle)-system are (2S,1D); (3S,2D,1G); (4S,...) and (5S,...) for p, d, ^{3}He and α particles respectively. The binding energies E_b between cluster and core should be taken from structure information. The values we used for the (^{24}Mg + particle)-system are

given in Table 2. The most direct information for the (^{24}Mg + d) system comes from the ^{24}Mg(α,d)^{26}Al reaction investigated by Rivet et al [12]. Using their level assignments it is encouraging that the bound states calculated for 3S, 1G and 1H configurations provide at least comparable well depths (see Table 2), although spin orbit and residual interactions were completely neglected.

The binding energies E_b between cluster and core are, of course, sensitive to the internal binding energy of the cluster. Using instead of E_b the value of E_b^{free} of the (^{24}Mg+$\sum$nucleon)-system we obtain bound state potentials which follow the sum rule (Table 1). The cluster wave functions are, because of their shorter wave length, more sensitive to the volume of the potential than the proton wave function. Therefore it is not surprising that the 'spherical' bound potential of the proton is deeper than $V_{d,^3He,\alpha}(E_b^{free})/n$ since it is determined to match the energy levels of the deformed nuclei ^{25}Al and ^{23}Na (see (d,^{3}He) reaction) respectively.

The calculated 'right' 3S, 4S and 5S bound state potentials for the d, ^{3}He and α clusters respectively are generally a little larger than the corresponding 'right' scattering potentials, which is, of course, to be expected from the energy dependence of potentials. $V_b(E_b^{free})$, however, is much deeper than the scattering potentials. This is particularly true for the α potentials at 81 and 120 MeV bombarding energy indicating that the scattering potentials are reduced in strength because of the internal saturation of nuclear forces within the cluster. However, much more investigation is needed because of the difficulty of extrapolating the scattering potentials back to zero bombarding energy and remaining in the 'right' potential family.

For transfer reactions like the ^{24}Mg(d,^{3}He)^{23}Na or the ^{26}Mg(p,t)^{24}Mg reactions the relationship between the bound state and the scattering wave functions is of considerable importance and the depth of the bound state potentials may determine the choice of best fitting potentials [13]. Stock et al [14] have shown that the assumptions made within the simple DWBA theory for calculating the cross section of the reaction

$$a + (C + b) \rightarrow (a + b) + C$$

involve:

$$V_{aC} \simeq U_i \quad \text{and} \quad V_{aC} + V_{bC} \simeq U_f$$

where C stands for the core of the target nucleus, $U_{i,f}$ are the potentials

generating the distorted waves and V are the actual interaction potentials. Interpreting V_{bC} as the bound state potential well depth of the transferred particle (cluster) we obtain the sum rule for reactions

$$U_i + V_{bound} \simeq U_f \ .$$

Since the bound state potentials are real, we apply this sum rule only to the real parts of the potentials and use the measured imaginary parameters. In Table 3 we have collected the potential well depths for a few representative transitions of the $^{24}Mg(d,^3He)^{23}Na$ and the $^{26}Mg(p,t)^{24}Mg$ reactions.

Fig. 3 shows the data for the pick up reactions and the cross sections for measured and constructed potentials (code Julie).[10] The (p,t) angular distributions are the data measured by Cosper et al [15]. The constructed ^3He (triton) potentials are obtained by substituting the real potential depth V by V_{CON} according to Table 3, the labeling Con 4/Con 5 meaning that all other parameters are those from the measured 4S and 5S ^3He potentials respectively.

The $^{24}Mg(d,^3He)^{23}Na$ experimental cross sections are not fitted by the measured 3S/4S potential combination. The ℓ=1 distribution, however, is apparently the closest fitted, corresponding to the fact that V_{CON} (ℓ=1) is closest in depth to the measured 4S-^3He potential. A larger bound state radius of r_o=1.35 slightly improves the DWBA cross section (upper curve). The 3S/5S potential combination fits the (d,^3He) cross section fairly well. It is the usual 'Bassel combination' of potentials. The 3S/CON4,CON5 combinations, however, fit the data equally well, the magnitude of calculated cross sections being similar to that of the 3S/5S combination (see normalization constants M). The same behavior is found for the $^{24}Mg(d,t)^{23}Mg$ reaction.

Inspecting the (d,^3He) fits in more detail, we see that the ℓ=1 distribution is fairly well reproduced, whereas the ℓ=0, 2 data are not exactly in phase with the DWBA curves for either the measured or the constructed potentials. This discrepancy is even stronger in the $^{24}Mg(^3He,\alpha)^{23}Mg$ reaction [4] and cannot be removed by changing the bound state radius or using deformed bound state wave functions [16]. An increase of all radii of the scattering potentials by 12% yields good fits for the single nucleon pick up reactions from the deformed s, d shell whereas the ℓ=1 distributions (pickup from the

core) are fitted by measured parameters.

In the lower part of Fig.3 we show the results for the $^{26}Mg(p,t)^{24}Mg$ reaction. The calculated cross sections were obtained from code Julie using 3S and 2D cluster bound state wave functions for the $\ell=0$ and $\ell=2$ transitions respectively. Contributions from other node numbers should be small[20] and were neglected. We used the ^3He potentials for the tritons and took the proton potential obtained for 50 MeV scattering[7] which includes a spin orbit potential V_{so}. However, our 'systematic' 2S proton potential obtained from the 30.5 MeV data (without V_{so}) fits the (p,t) cross sections almost equally well and gives the same results concerning ratios of intensities.

Obviously the constructed potentials fit the (p,t) data remarkably well. Comparing with the measured 2S/5S potential combination the most important difference is the change in the relative magnitude of calculated cross sections for the $\ell=0$ transitions to the T=0 ground state and the T=2, 15.43 MeV state in ^{24}Mg (see normalization constants M). Assuming pure $(d_{5/2})^n$, seniority v=0 states the ratio of normalization constants should be given by:

$$\frac{M(T=2)}{M(T=0)} = \frac{C^2_{T=2} \cdot cfp(T=2)^2}{C^2_{T=0} \cdot cfp(T=0)^2} = \frac{2}{7}$$

where C_T is the isospin Clebsch Gordan coefficient. The fractional parentage coefficients for separating two nucleons from the target nucleus were taken from Towner and Hardy[17]. The expected ratio is very close to the experimental ratio of 0.30 ± .03 obtained from the constructed potentials, whereas the 2S/5S measured potentials yield 0.17 ± .03 (averaged values for different proton potentials). This change in ratios of intensities emphasizes the importance of selecting proper optical potentials.

We wish to thank Dr.C.J.Hardy for valuable discussions and Mary F.Reed for allowing us to use her $^{24}Mg(\alpha,\alpha)^{24}Mg$ data prior to publication.

REFERENCES

1) The potential sum rule has been investigated mostly for deuteron potentials, see e.g., S. Watanabe, Nucl. Phys. 8 (1958) 288; J. Testoni and L. C. Gomes, Nucl. Phys. 89 (1966) 288; E. Coffou and L. J. B. Goldfarb, Nucl. Phys. A94 (1967) 241; F. G. Perey and G. R. Satchler, Nucl. Phys. A97 (1967) 515

2) The sum rule for potentials is known to minimize corrections for zero range, local energy DWBA stripping cross sections, see P. J. A. Buttle and L. J. B. Goldfarb, Proc. Phys. Soc. 83 (1964) 701; J. K. Dickens, R. M. Drisko, F. G. Perey and G. R. Satchler, Phys. Letters 15 (1965) 337

3) R. K. Cole, J. Eenmaa, S. M. Scarrot and C. N. Waddel; USC-Report No. 136-114 (1966)

4) H. H. Duhm, B. G. Harvey, D. Hendrie, J. Saudinos, J. Mahoney, B. Parkinson and N. Jarvis, to be published

5) M. Reed, private communication; D. L. Hendrie, B. G. Harvey, J. Mahoney, and J. R. Meriwether, BAPS 12 (1967) 555; M. F. Reed, B. G. Harvey, and D. L. Hendrie BAPS 12 (1967) 912

6) Modified version of Seek, by M. A. Melkanoff, J. Raynal, and T. Sawada, UCLA-Report No. 66-10 (1966)

7) E. J. Burge, M. Calderbank, J. A. Fannon, V. E. Lewis, A. A. Rush, D. A. Smith, N. K. Ganguly, RHEL-Report No. R136 (1966)

8) B. Duelli, F. Hinterberger, G. Mairle, U. Schmidt-Rohr, P. Turek and G. Wagner, Phys. Letters 23 (1966) 485

9) R. M. Drisko, G. R. Satchler, and R. H. Bassel, Phys. Letters 5 (1963) 347

10) R. H. Bassel, R. M. Drisko, and G. R. Satchler, ORNL-report no. 3240 (1962)

11) T. A. Brody and M. Moshinsky, Tables of Transformation Brackets, Monografias del Instituto de Fisica, Mexico, 1960

12) E. Rivet, R. H. Pehl, J. Cerny, and B. G. Harvey, Phys. Rev. 141 (1966) 1021

13) DWBA cross sections are known to be sensitive to the choice of parameter families, see e.g., J. R. Rook, Nucl. Phys. 61 (1965) 219; H. H. Duhm, R. Bock, P. David, and U. Lynen, Proc. of the Gatlinburg Conf. 1966

14) R. Stock, R. Bock, P. David, H. H. Duhm, and T. Tamura, to be published

15) S. W. Cosper, H. Brunnader, J. Cerny, R. L. Mc Grath, Phys. Letters 25B (1967) 324

16) E. Rost, Phys. Rev. 154 (1967) 994

17) J. S. Towner and C. J. Hardy, to be published

18) J. S. Vincent, E. T. Boschitz, and J. R. Priest, Phys. Letters 25B (1967)81
J. M. Naqib and J. S. Blair, to be published

19) J. Kokame, F. Fukunaga, H. Nakamura, and N. Inoue, Phys. Letters 8 (1964) 342

20) N. K. Glendenning, Phys. Rev. 137 (1965) B102

Table Captions

Table 1. Bound state and scattering potentials for ^{24}Mg. The proton potentials including a spin-orbit potential were taken from Ref. 7 and 3. $V(E_b^{free})$ for protons which are labelled by an asterisk were obtained by averaging $V_{d,^3He,\alpha}(E_b^{free})/n$, where n is 2, 3 and 4 respectively. Potentials are given in MeV and radii in units of Fermi.

Table 2. Binding energies E_b and E_b^{free} for various cluster configurations of the (^{24}Mg + particle)-system. The bound state potentials $V(E_b)$ obtained for the (^{24}Mg + d) system are given at the bottom. Energies (potentials) are given in MeV and radii in units of Fermi.

Table 3. Sum rule potential depths V_{CON} for various levels observed in the ^{24}Mg(d, ^{3}He)^{23}Na and ^{26}Mg(p,t)^{24}Mg reactions.

Table 1

bound state potentials					optical model parameters								
E(MeV)		config.	$V_b(E_b^{free})$	$V_b(E_b)$	V	r_o	a	W_{vol}	r_w	a_w	V_{so}	r_{so}	a_{so}
50.0	p				43.6	1.09	.74	7.39	1.53	.533	5.34	.98	.55
30.5	p				41.5	1.19	.70	4.60	1.72	.52	6.6	1.19	.70
											X^2		
30.5	p	2S	42.2*	51.5	41.6	1.2	.65	4.23	1.7	.59	3.2		
40.0	d	3S	83.6	79.4	70.2	1.2	.75	12.3	1.7	.80	13.6		
47.5	^{3}He	4S	123.0	111.2	95.5	1.2	.77	18.4	1.7	.84	40.6		
35.0				111.4	94.9	1.2	.75	17.0	1.7	.84	34.6		
119.7	α	5S	173.2	122.0	111.8	1.2	.83	18.6	1.7	.70	4.4		
35.0	^{3}He	5S	169.8	151.2	151.5	1.2	.66	29.6	1.3	1.11	40.1		
30.5	p	2S	51.9*	64.8	54.1	1.0	.79	3.76	1.8	.56	13.9		
40.0	d	3S	104.7	99.6	86.6	1.0	.83	9.89	1.8	.82	8.5		
47.5	^{3}He	4S	152.8	135.8	119.9	1.0	.88	15.9	1.8	.76	16.4		
35.0			153.2	136.5	120.7	1.0	.85	14.8	1.8	.79	20.4		
119.7	α	5S	212.5	150.4	135.3	1.0	.96	14.1	1.8	.68	6.6		
40.0	d	4S	167.9	162.2	173.6	1.0	.70	12.0	1.6	.98	12.1		
47.5	^{3}He	5S	213.4	195.5	197.8	1.0	.76	21.2	1.6	.91	22.9		
35.0					192.0	1.0	.76	21.0	1.6	.91	32.6		
119.7	↑ α	5S	160.4	112.6	100.0	1.28	.78	23.8	1.6	.71	1.65		
81.0			146.0	102.4	100.0	1.38	.69	31.7	1.6	.58	6.4		
65.7			138.7	96.7	100.0	1.44	.66	40.1	1.6	.48	19.0		
50.1			134.3	94.3	100.0	1.47	.58	27.6	1.6	.47	57.0		
119.7	↓		144.1	100.2	76.8	1.40	.73	41.9			18.8		
81.0			143.6	100.4	89.7	1.40	.69	47.0			6.2		
65.7			143.3	100.5	94.0	1.40	.67	44.8			25.1		
50.1			142.4	100.9	111.9	1.40	.60	38.9			62.2		

Table 2

config.		levels	center of gravity (assumed)	E_b	E_b^{free}
^{25}Al: (^{24}Mg + p)	2S	ℓ=0, $1/2^+$ 0.45, 2.50	1.2	1.08	1.08
	3S	ℓ=0, 1^+ 1.06	2.4	9.0	11.2
^{26}Al: (^{24}Mg + d)	1G	ℓ=4, 5^+ 0.00	0.0	11.4	13.2
	1H	ℓ=5, 6^- 6.95	6.95	4.46	6.7
^{27}Si:(^{24}Mg + ^3He)	4S	ℓ=0, $1/2^-$ 0.78, 3.54?	2.0	11.38	19.1
^{28}Si; (^{24}Mg + α)	5S	ℓ=0,, 0^+ 0.00, 4.97	0.0	9.98	38.2

	r_o	a	V_b(3S)	V_b(1G)	V_b(1H)
(^{24}Mg + d)	1.2	.75	79.4	84.0	94.3
	1.0	.83	99.6	111.6	128.8

Table 3

r_o=1.2, r_c=1.3	a=.65	a=.75	a=.75
Ex(^{23}Na)	V^{p}_{bound}	$V^{d}_{scatt.}$	$V^{^3He}_{CON}$
2.39 ℓ = 0	76.5		146.7
0.44 ℓ = 2	71.5	70.2	141.5
3.68 ℓ = 1	53.1		123.3
Ex(^{24}Mg)	$V^{p}_{scatt.}$	V^{2n}_{bound}	V^{t}_{CON}
0.00 ℓ = 0		87.3	128.9
1.37 ℓ = 2	41.6	89.6	131.2
15.43 ℓ = 0		112.4	154.0

Figure Captions

Fig. 1. Angular distributions for p, d, ^{3}He and α particles elastically scattered by ^{24}Mg. Optical model parameters from Table I (see text).

Fig. 2. X^2 - Minima in the (V, r_o) plane for p, d, ^{3}He and α potentials for ^{24}Mg. The lines labelled by (1...7S) are bound state potential well depths of cluster wave functions with a different number of nodes.

Fig. 3. Characteristic angular distributions from the ^{24}Mg(d, ^{3}He)^{23}Na and ^{26}Mg(p,t)^{24}Mg reactions. The DWBA cross sections are obtained from measured and constructed potentials. Note that the data are adjusted to the DWBA curves, the normalization M being the ratio of experimental to calculated cross section.

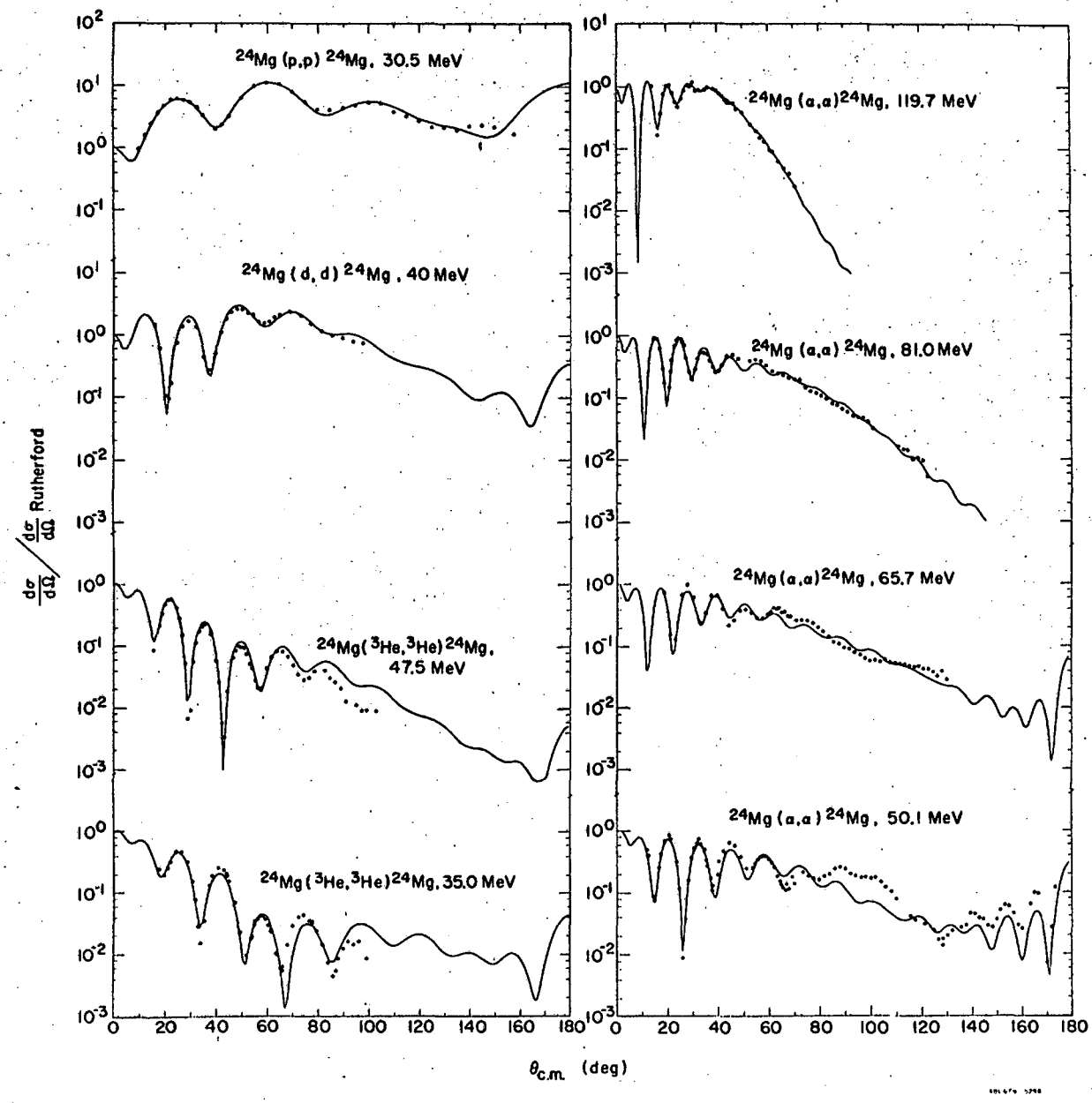

XBL 679-5298

Fig. 1

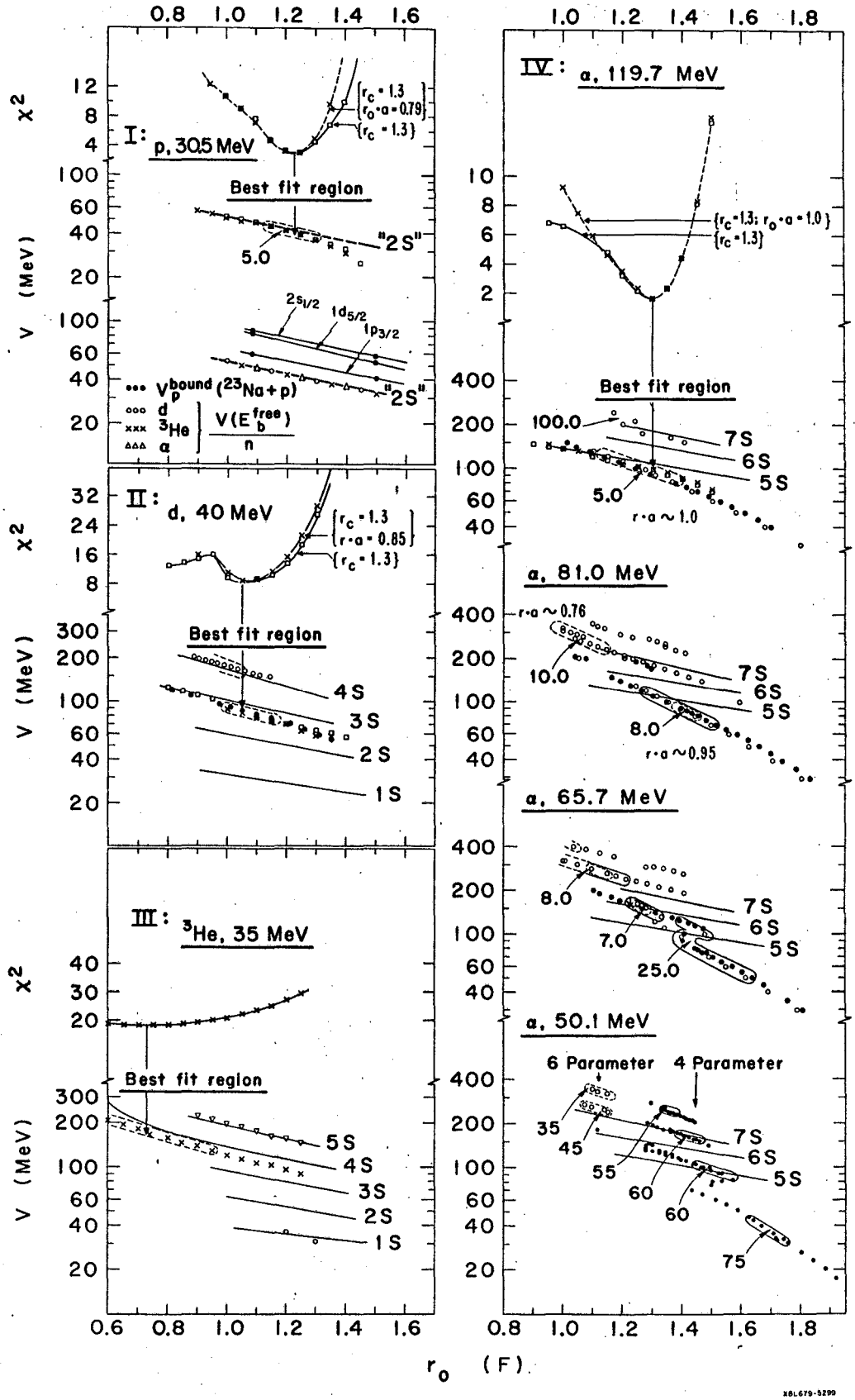
I: p, 30.5 MeV
Best fit region
"2S"
5.0
2s1/2
1d5/2
1p3/2
V (MeV)
χ²
II: d, 40 MeV
Best fit region
4S
3S
2S
1S
III: 3He, 35 MeV
Best fit region
5S
4S
3S
2S
1S
IV: α, 119.7 MeV
Best fit region
100.0
7S
6S
5S
5.0
r·a ~ 1.0
α, 81.0 MeV
r·a ~ 0.76
10.0
8.0
r·a ~ 0.95
α, 65.7 MeV
8.0
7.0
25.0
α, 50.1 MeV
6 Parameter
4 Parameter
35
45
55
60
60
75
r0 (F)

Fig. 2

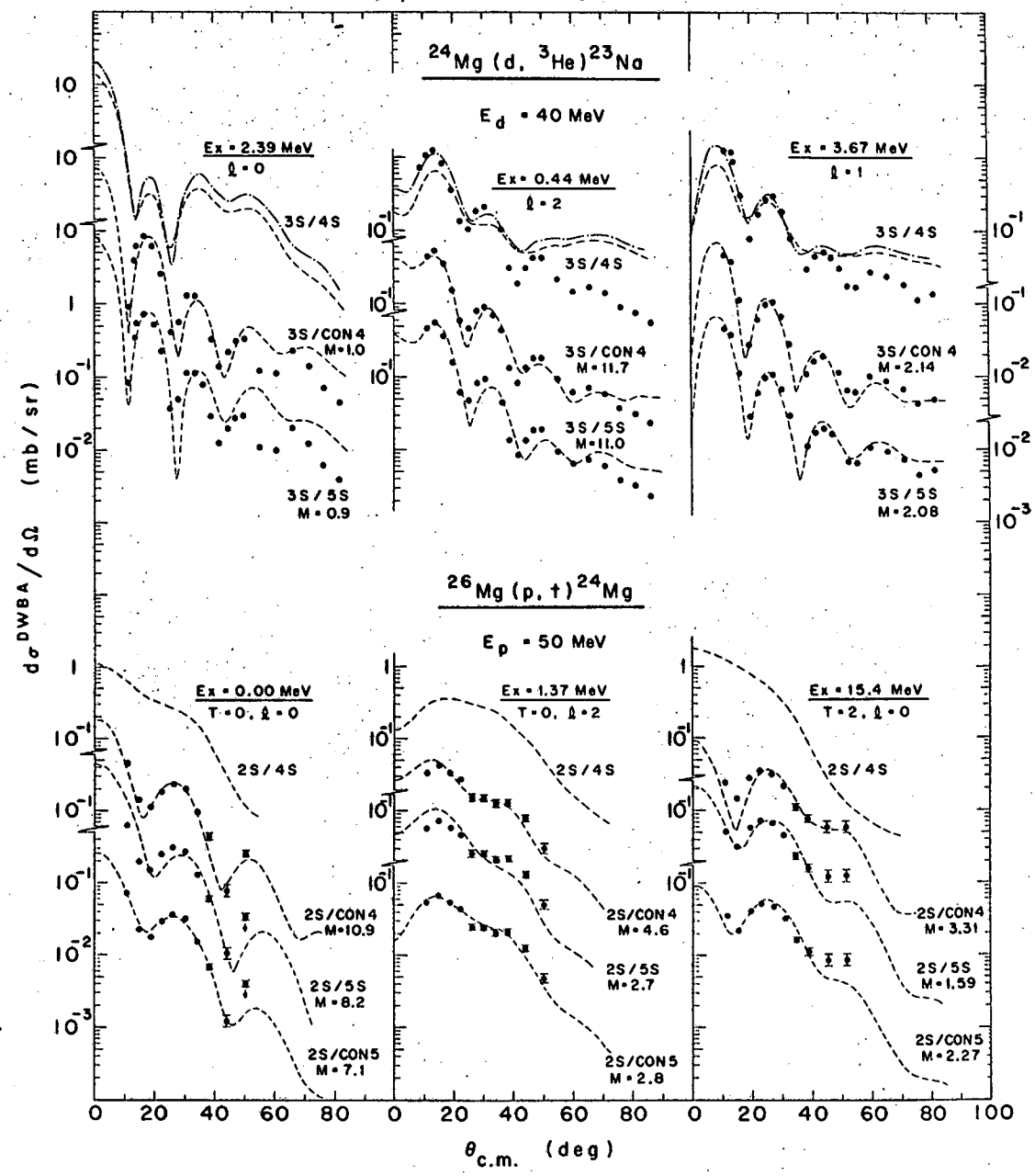

XBL 670-5322

Fig. 3